https://doi.org/10.5194/angeo-2019-133
Preprint. Discussion started: 25 October 2019


Annales Geophysicae Discussions

# Structural characterization of the equatorial F region plasma irregularities in the multifractal context

Neelakshi Joshi[1], Reinaldo R. Rosa[1], Siomel Savio[2,4], Esfhan Alam Kherani[2], Francisco Carlos de Meneses[3,4], Stephan Stephany[1], and Polinaya Muralikrishna[2]

[1]Computational Space Physics Group, Lab for Computing and Applied Math (LABAC), National Institute for Space Research (INPE), Av. dos Astronautas, 1758, São José dos Campos, São Paulo 12227-690, Brazil
[2]Aeronomy Division, National Institute for Space Research (INPE), Av. dos Astronautas, 1758, São José dos Campos, São Paulo 12227-690, Brazil
[3]School of Physics and Mathematics, Autonomous University of Nuevo León (UANL), Av. Universidad s/n, Cd. Universitaria, San Nicolás de los Garza, N.L. 66455, Mexico
[4]China-Brazil Joint Laboratory for Space Weather, NSSC/INPE, Av. dos Astronautas, 1758, São José dos Campos, São Paulo 12227-690, Brazil

**Correspondence:** Neelakshi J. (neelakshij@gmail.com)

**Abstract.** In the emerging ionosphere-space-weather paradigm, investigating dynamical properties of ionospheric plasma irregularities using advanced computational non-linear algorithms is providing new insights into their turbulent-like nature, for instance, the evidence of energy distribution via multiplicative cascade. In this study, we present multifractal analysis of the equatorial F region *in situ* data obtained from two different experiments performed at Alcântara (2.4°S; 44.4°W), Brazil to explore their scaling structures. First experiment observed several large-medium scale plasma bubbles whereas second experiment observed vertical uplift of the base of F region. Multifractal detrended fluctuation analysis and p-model fit is used to analyze the plasma density fluctuation time series. Result shows presence of multifractality with degree of multifractality $0.53 - 0.93$ with $0.3 \leq p \leq 0.4$ cascading probability for first experiment. Another experimental data also exhibits multifractality with degree of multifractality $0.19 - 0.27$ with $0.42 \leq p \leq 0.44$ cascading probability in the ionospheric plasma irregularities. Our results confirm the nonhomogeneous nature of plasma irregularities and characterize the underlying nonhomogeneous multiplicative cascade hypothesis in the ionospheric medium. Differences in terms of scaling and complexity in data belonging to different types of phenomena are also addressed.

## 1 Introduction

Present ionospheric research is transiting towards ionospheric space weather that goes beyond the ground- and space-based communication interruptions to influence decision making communities on social, economical, and physical infrastructural policies. The enhancements in the ionospheric plasma irregularities driven by space weather conditions demand an accurate characterization of the dynamical properties of the electron density and its complex nonlinear variation (Cander L. R., 2019). With instruments operating over substantial frequency domain, study of plasma density irregularities provide insight into the underlying physical mechanism and its structural properties (Wernik et al., 2003; Muralikrishna et al., 2003). Energy dissipa-

https://doi.org/10.5194/angeo-2019-133
Preprint. Discussion started: 25 October 2019


Annales Geophysicae Discussions

tion is found to be an underlying process for the occurrence of electron density or electric field fluctuations in the ionospheric plasma irregularities (Jahn and LaBelle, 1998; Kelley and Hysell, 1991). Spectral analysis though widely used, falls short in characterizing nonstationary data as they assume stationarity in the data, which is equivalent to presuming homogeneous turbulence; hence, more robust method is necessary to analyze nonstationary data (Wernik et al., 2003). In addition, to develop a robust specification and a forecasting model, along with classical morphological, statistical and spectral studies, a thorough understanding of nonlinearity in the ionospheric irregularities is essential (Tanna and Pathak, 2014). Various different approaches had been explored to understand nonlinear characteristics and intermittency in the ionospheric irregularities, like structure function analysis (Dyrud et al., 2008), fractal and multifractal analysis (Wernik et al., 2003; Alimov et al., 2008; Bolzan et al., 2013; Tanna and Pathak, 2014; Miriyala et al., 2015; Chandrasekhar et al., 2016; Fornari et al., 2016; Sivavaraprasad et al., 2018; Neelakshi et al., 2019), multispectral optical imaging (Chian et al., 2018).

Detrended fluctuation analysis (DFA; Peng et al. (1994)) has been a proven successful method to find power law correlation and monofractal scaling in noisy, nonstationary data. The DFA is a robust method as it can handle discontinuous and lengthwise short data. In case data is more complex and has intricate scaling, various scaling exponents characterize different parts of the data. To characterize such multiple scaling behavior in the data, Kantelhardt et al. (2002) generalized the DFA to multifractal detrended fluctuation analysis (MFDFA), and have shown the equivalence to standard partition function based multifractal method for stationary data with compact-support.

The MFDFA has wide applications in many branches of sciences - medicine (Makowiec, 2011), physics (Freitas et al., 2016), engineering (Lu et al., 2016), finance (Grech D., 2016) and social sciences (Kantelhardt, 2009; Telesca and Lovallo, 2011) - to understand the complexity of the system through its scaling exponents that characterize multifractal dynamics of the system. The MFDFA has been applied to study ionospheric scintillation index time series (Tanna and Pathak, 2014; Miriyala et al., 2015) and ionospheric total electron content data (Chandrasekhar et al., 2016; Sivavaraprasad et al., 2018). In analogy, wavelet transform is applied to study ionospheric irregularities (Wernik et al., 2003; Bolzan et al., 2013). These analyses identified multifractality and intermittency in the nonlinear ionospheric irregularities.

In this work, we explore low latitude equatorial F region emphin situ data obtained from two different experiments, and performed from the same rocket launching station. First experiment, done on 18 December 1995, is chosen as the rocket traversed through various large-medium scale plasma irregularities during its descent, which were associated with the generalized Rayleigh-Taylor instability (Muralikrishna et al., 2003). Whereas the second experiment, done on 8 December 2012, is chosen as during the experiment the base of F region was moving upward, i.e. pre-reversal enhancement (PRE) of vertical plasma drift was observed (Savio et al., 2016; Savio Odriozola et al., 2017).

In equatorial ionosphere, the evening PRE is considered as an important seeding mechanism for post sunset F region irregularities, as quick and acute uplift of the electric field escalates the rate of growth of the generalized Rayleigh-Taylor instability (Li et al., 2007; Kelley et al., 2009; Abdu et al., 2018). Knowing the relation between these two phenomena, it will be interesting to know the differences in their scaling behavior and complexity. Investigating these plasma fluctuations may enable to study the scaling properties of these plasma irregularities, and also knowing various characteristics along with the complexity of data may provide important inputs to model empirical data. Hence, we apply the MFDFA method to plasma density fluctuation

https://doi.org/10.5194/angeo-2019-133
Preprint. Discussion started: 25 October 2019


Annales Geophysicae Discussions

data obtained from these two different *in situ* experiments. To corroborate our results, the singularity spectrum obtained from the MFDFA is fitted with a p-model (Meneveau and Sreenivasan, 1987) based on the generalized two-scale Cantor set. Details on the experiments are given briefly in section 2. Methods are described in section 3. Results of the analyses are discussed in section 4 followed by concluding remarks in section 5.

## 2 *in situ* experiments

The equatorial launching station of Brazil is located at Alcântara (2.24° S, 44.4° W, dip latitude 5.5°S). SONDA III rocket was launched at 21:17 LT, on December 18, 1995 under favourable conditions for formation of plasma bubble. During the $\sim$ 11 min flight, plane of rocket trajectory was almost orthogonal to the geomagnetic field lines, spanned $\sim$ 589 km distance horizontally with an apogee at altitude $\sim$ 557 km. Rocket-born electric field double probe (EFP) measured electric field fluctuations related with ionospheric plasma irregularities. In the upleg profile (ascent of the rocket), the F region base is clearly observed around 300 km, but without any large scale depletion or bubble. On the other hand, several plasma bubbles of large-medium scale were observed in the downleg profile (descent of the rocket), around the base of F region and also topside of it, but without any sharp indication of the F region base from altitude above 240 km. Rocket traversed through regions of different altitudes separated by a few hundreds of kilometers during upleg and downleg so this might elucidate the large differences observed in ascent and descent of the rocket (Muralikrishna et al., 2003; Muralikrishna P. and Abdu M. A., 2006; Muralikrishna P. and Vieira L. P., 2007). Detail explanation of *in situ* experiment and the analysis is found in Muralikrishna et al. (2003); Muralikrishna P. and Abdu M. A. (2006); Muralikrishna P. and Vieira L. P. (2007).

Some of the key results from the analysis indicate - (1) initiation of cascade process, owing to Rayleigh–Taylor instability mechanism, near the base of F region that resulted in the development of the plasma bubbles or large scale irregularities, and (2) subsequently, advecting energy to higher altitudes, smaller scale irregularities were observed, owing to Cross-Field instability mechanism (Muralikrishna et al., 2003; Muralikrishna P. and Abdu M. A., 2006; Muralikrishna P. and Vieira L. P., 2007).

From the same rocket launching station, Alcântara, a two-stage VS-30 Orion sounding rocket was launched at 19:00 LT, on December 8, 2012, under favorable conditions for strong spread-F. During the $\sim$ 11 min flight, the rocket trajectory was in the north-northeast direction towards magnetic equator, ranging $\sim$ 384 km horizontally with an apogee at $\sim$ 428 km. conical Langmuir probe (CLP) onboard the rocket measured electron density fluctuations associated with ionospheric plasma irregularities. In this experiment, the F region base was clearly observed in the downleg profile around 300 km, with some small scale fluctuations in the F region. Ground equipment, digisonde, near launching station, showed fast uplift of the F region base before sunset and its continuation for more than two hours, indicating possibility of pre-reversal enhancement of the vertical plasma drift (Savio et al., 2016). Further explanation of *in situ* experiment and data analysis is found in Savio et al. (2016); Savio Odriozola et al. (2017).

https://doi.org/10.5194/angeo-2019-133
Preprint. Discussion started: 25 October 2019


Annales Geophysicae Discussions

## 3 Methods

### 3.1 Multifractal detrended fluctuation analysis

Implementation of the MFDFA consists of first, compute the profile by integrating the time series and then divide it into non-overlapping and equidistant $N_s$ segments of length $s$, referred to as scales. These segments are then detrended using linear least squares. The variance is calculated over the all segments.

$$F^2(s,n) = \left( \frac{1}{s} \sum_{k=1}^{s} [y[(n-1)s+k] - y_n(k)]^2 \right) \tag{1}$$

Then followed by averaging the root mean square, the $q^{th}$ order fluctuation function is computed.

$$F_q(s) = \left( \frac{1}{N_s} \sum_{k=1}^{N_s} [F^2(s,n)]^{q/2} \right)^{1/q} \tag{2}$$

When $q = 0$, logarithmic averaging should be used to calculate fluctuation function,

$$F_0(s) = exp\left( \frac{1}{2N_s} \sum_{k=1}^{N_s} [ln(F^2(s,n))] \right) \tag{3}$$

Applying linear fit to the fluctuation function profile on log-log plot yields the generalized Hurst exponent, $h(q)$, for each moment $q$ as $F_q(s) \propto s^{h(q)}$. The computed generalized Hurst exponent $h(q)$ can be related to the classical multifractal scaling (or mass) exponent as $\tau(q)$ by $\tau(q) = qh(q) - 1$. Singularity (or multifractal) spectrum is calculated using $h(q)$ where $\alpha$ represents singularity strength and $f(\alpha)$ represents set of multifractal dimensions:

$$\alpha = h(q) + qh'(q) \tag{4}$$

$$f(\alpha) = q(\alpha - h(q)) + 1 \tag{5}$$

Detailed implementation can be found in Kantelhardt et al. (2002).

### 3.2 p-model

The p-model is proposed by Meneveau and Sreenivasan (1987) to model energy cascading process in the inertial range of fully developed turbulence for the dissipation field. The p-model starts with a coherent structure with an assumed specific energy flux per unit length which then undergoes a binary fragmentation at each cascading step, distributing the energy flux with probabilities $p1\&p2$ among the fragments $l1\&l2$. Based on the generalized two-scale Cantor set, the p-model consider equal scales ($l1 = l2$) and unequal weights ($p1 \neq p2$ and $p1 + p2 \leq 1$). When $p1 + p2 \leq 1$, loss in $p$ parameter given by $dp =$

https://doi.org/10.5194/angeo-2019-133
Preprint. Discussion started: 25 October 2019


Annales Geophysicae Discussions

$1-p1-p2$, accounts for the direct energy dissipation in the energy cascading process in the inertial range. The proposed p-model claims to display all multifractal properties of one-dimensional section of dissipation field for fully developed turbulence. Multifractality ceases to exist for $p = 0.5$. Analytical formulation for the generalized two scale Cantor set is given by

$$\alpha = \frac{lnp1 + (n/m-1)lnp2}{lnl1 + (n/m-1)lnl2} \tag{6}$$

$$f(\alpha) = \frac{(n/m-1)ln(n/m-1) - (n/m)ln(n/m)}{lnl1 + (n/m-1)lnl2} \tag{7}$$

is useful to determine the generalized multifractal dimensions which represents the singularity spectrum. (Halsey et al., 1986).

## 4 Results and Interpretation

Six time series of *in situ* observations of electric field fluctuations from the F region are selected from the first experiment performed on 18 December 1995, corresponding to the mean heights of $264.58, 270.22, 292.37, 324.00, 358.56$, and $429.65$ km in downleg. Similarly from the second experiment performed on 12 December 2012, we selected three time series of electron density fluctuations from F region, corresponding to the mean heights of $339.94, 348.99$,and $400.24$ km in downleg. These time series are subjected to multifractal analysis. Primarily, the profile is obtained by differencing the time series i.e. $y = x(i+1) - x(i)$, using the criterion based on the power exponent obtained in the DFA method, prescribed by (Ihlen E. (2012), Table 2) for biomedical time series to yield best results from the MFDFA method. We found the criterion to hold for ionospheric *in situ* data under study. Scales upto one tenth of the length of the time series are considered. From the MFDFA, the generalized Hurst exponent, $h(q)$, classical multifractal scaling exponent $\tau(q)$ and singularity spectrum $\alpha$ and $f(\alpha)$ are obtained. We show comprehensive analysis for only one time series from each of the two experiments (Figures 1 and 3). For remaining time series, we show only singularity spectrum along with its respective time series (Figures 2, 4), but we report the analysis of both experiments in Tables 1 and 2 respectively.

In the MFDFA, smaller scales identify rapid variations while large scales identify slow variations in time series. In order to characterize all types of fluctuations, scale should be varied across all size range i.e., from small to large sizes. Positive $q$ describe intense fluctuations larger than average whereas negative $q$ represent region of the fluctuations lower than average. For positive $q$, $h(q)$ illustrates the scaling behaviour of segments (scales) influenced by large fluctuations and are described by smaller scaling exponent values of $h(q)$, while for negative $q$, scaling behaviour of segments (scales) influenced by small fluctuations are characterized by $h(q)$ and are described by larger scaling exponent values of $h(q)$. To outline, for a multifractal time series $h(q)$ monotonically decreases with $q$, and $\tau(q)$ shows nonlinear dependence on $q$.

Shape and width of the multifractal spectrum are also important measures to quantify the nature of multifractality present in data. If shape of the spectrum is left truncated, it indicates that the spectrum is insensitive to larger local fluctuations, which is characterized by positive values of $q$. On the other hand, if shape of the spectrum is right truncated, it indicates that the spectrum is insensitive to smaller local fluctuations, which is characterized by negative values of $q$. Width of the spectrum infers

https://doi.org/10.5194/angeo-2019-133
Preprint. Discussion started: 25 October 2019


Annales Geophysicae Discussions

the degree of multifractality and complexity of data. Degree of multifractality, $\Delta\alpha$, is the difference between maximum and minimum dimension, represent the deviation from average fractal structure, and directly relate to the parameters corresponding to multiplicative cascade process. Larger (smaller) value of $\Delta\alpha$ infers stronger (weaker) multifractality in data.

$$\Delta\alpha = \alpha_{max} - \alpha_{min} \tag{8}$$

Alongside $\Delta\alpha$, measure of asymmetry, $A$, is given by

$$A = \frac{\alpha_0 - \alpha_{min}}{\alpha_{max} - \alpha_0} \tag{9}$$

where the singularity strength, $\alpha_0$, corresponds to the maximum value of the singularity spectrum i.e., for $f(\alpha_0) = 1$. When $A = 1$, singularity spectrum is symmetric in a sense that the time series is influenced with both the coarser as well as fine structures. When $A > 1$, the spectrum is left-skewed which implies that the time series is more influenced with the coarser structures (large fluctuations). When $A < 1$, the spectrum is right-skewed which implies that the time series is more influenced with fine structures (small fluctuations).

Figure 1 shows detailed multifractal analysis of a time series from first experiment, corresponding to the mean height of 324.00 km (top left). The profile of $h(q)$ as a function of $q$ is shown on the top right, and of $\tau(q)$ on the bottom left. The corresponding singularity spectrum is shown on the bottom right panel. The spectrum is right-skewed, indicating the influence of the negative values of $q$ on the data. It is evident as well from the $h(q)$ profile. The variation of $h(q)$ for negative $q$ is observed to be comparatively steep. The plot for $\tau(q)$ versus $q$ shows marked deviation from linearity, asserting the presence of the multifractality in time series for the chosen height. In addition to the derived inferences from the visual analysis of the singularity spectrum reported above, multifractal measures, $\Delta\alpha$ and $A$, can be quantified (eqs. 8 & 9). The measure $A = 0.32$ quantifies the skewness while $\Delta\alpha = 0.72$ infers strength of multifractality. These two measures are listed in Table 1. Lastly, the singularity spectrum is fitted with a p-model (shown with a continuous line), where the scales are equal i.e., $l1 = l2 = 0.5$ and the weights, $p1$ and $p2$, are varied such that $p1 + p2 \leq 1$. Nevertheless, loss in $p$ parameter had to be accounted to obtain an optimal fit. The loss factor, $dp$, signifies non-conservative energy distribution i.e., a dissipative energy cascading process in the inertial range. We have obtained a dissipative factor of $0.090$, with $p1 = 0.315$. The p-model fit parameters are listed in Table 1.

Similar to Figure 1, Figure 3 shows detailed multifractal analysis of a time series from second experiment, corresponding to the mean height of 339.94 km (top left). The profile of $h(q)$ as a function of $q$ is shown on the top right, and of $\tau(q)$ on the bottom left. The corresponding singularity spectrum is shown on the bottom right panel. The spectrum is left-skewed, indicating the influence of the positive values of $q$ on the data. The variation of $h(q)$ for positive $q$ is observed to be comparatively steep. The plot for $\tau(q)$ versus $q$ show marked deviation from linearity, asserting the presence of the multifractality in the time series for the chosen height. The multifractal measures computed, $A = 1.34$ and $\Delta\alpha = 0.27$, and listed in Table 2. Lastly, the singularity spectrum is fitted with a p-model (shown with a continuous line). We have obtained a dissipative factor of $0.012$, with $p1 = 0.423$. The p-model fit parameters are listed in Table 2.

It is seen from above discussion that the singularity spectrum is sufficient to assess the multifractal nature, henceforth we show time series and the corresponding singularity spectrum for the remaining chosen heights. Figure 2 shows time series

https://doi.org/10.5194/angeo-2019-133
Preprint. Discussion started: 25 October 2019


Annales Geophysicae Discussions

selected from first experiment in the left panel and the corresponding singularity spectra in the right panel. For the time series corresponding to the mean height of $264.58$ km, singularity spectrum is slightly right skewed, which can be inferred from the measure $A = 0.82$. It indicates the influence of negative moments $q$ which characterizes smaller fluctuations than average. Degree of multifractality, $\Delta\alpha = 0.53$. The optimal p-model fit is obtained with parameters $p1 = 0.364$ and $dp = 0.059$. For the time series corresponding to the mean height of $270.22$ km, singularity spectrum is slightly left skewed, which can be inferred from the measure $A = 1.11$. It indicates the influence of positive moments $q$ which characterize intense larger fluctuations than average. Degree of multifractality, $\Delta\alpha = 0.82$. The optimal p-model fit is obtained with parameters $p1 = 0.34$ and $dp = 0.065$.

For the time series corresponding to the mean height of $292.37$ km, singularity spectrum is left skewed, reflected in the measure, $A = 2.99$. It indicates the influence of positive moments $q$ which characterize intense larger fluctuations than average. Besides, the spectrum is observed to be right truncated, implying negative values of q to be insensitive in characterizing fluctuations in the data. Degree of multifractality, $\Delta\alpha = 0.93$. The optimal p-model fit obtained with parameters $p1 = 0.339$ and $dp = 0.02$. We could fit spectrum corresponding to positive values of $q$. For the time series corresponding to the mean height of $358.56$ km, singularity spectrum is right skewed, reflected in measure $A = 0.37$. It indicates the influence of negative moments $q$ which characterize smaller fluctuations than average. Besides, the spectrum is observed to be left truncated, implying positive values of q to be insensitive in characterizing fluctuations in the data. Degree of multifractality, $\Delta\alpha = 0.52$. The optimal p-model fit obtained with parameters $p1 = 0.36$ and $dp = 0.07$. Finally, for the time series corresponding to the mean height of $429.65$ km, singularity spectrum is right skewed, also reflected in measure $A = 0.51$. It indicates the influence of negative moments $q$ which characterize slower varying fluctuations than average. Besides, the spectrum is observed to be left truncated, implying positive values of q are insensitive to characterize fluctuations in the data. Degree of multifractality is $\Delta\alpha = 0.28$. The optimal p-model fit obtained with parameters $p1 = 0.399$ and $dp = 0.0355$.

Figure 4 shows time series selected from second experiment in the left panel and corresponding singularity spectra in the right panel. For the time series corresponding to the mean height of $348.99$ km, singularity spectrum is left skewed, reflected in measure, $A = 1.72$. It indicates the influence of positive moments $q$ which characterize intense larger fluctuations than average. Degree of multifractality, $\Delta\alpha = 0.22$. The optimal p-model fit obtained with parameters $p1 = 0.43$ and $dp = 0.006$. For the time series corresponding to the mean height of $400.24$ km, singularity spectrum is almost symmetrical. This is reflected in measure, $A = 0.94$ which is very close to 1. It indicates both negative and positive moments $q$ characterize larger and smaller fluctuations than average almost equally. Degree of multifractality, $\Delta\alpha = 0.19$. The optimal p-model fit obtained with parameters $p1 = 0.4335$ and $dp = 0.01$.

## 5 Concluding remarks

Analysis using the Power Spectral Density (PSD) has been a norm in studying the *in situ* measurements of the ionospheric irregularities. It is established that energy dissipation is the underlying mechanism responsible for the occurrence of electron density or electric field fluctuations in the ionospheric plasma irregularities. Studying the morphology of these sites using the Fourier spectrum has some caveats in addressing the nonhomogeneous turbulence that introduces nonstationarity. Recent

https://doi.org/10.5194/angeo-2019-133
Preprint. Discussion started: 25 October 2019


Annales Geophysicae Discussions

advances in the computational algorithms based on fractal formalism, supplemented with mathematical model derived from probabilistic measures have conclusively substantiated the occurrence of energy cascading process in turbulent sites in the solar and interplanetary environment as well as in the laboratory using Kolmogorov's formalism as the basis (Macek W. M., 2007; Wawrzaszek A. and Macek W., 2010; Wawrzaszek et al., 2019).

In this work, we investigate the *in situ* F region electron density and electric field measurements obtained from past two experiments carried near equatorial sites in Brazil using MFDFA to understand the complexity of the data and to identify the signature of multiplicative energy cascade in the irregularities present there. We selected altogether *nine* time series at altitudes supposedly in or near the irregularities. In all the time series, we obtained $1.5 > h(q) > 0.9$, which indicate a long range correlation with persistent temporal fluctuations. In addition, we note that the $h(q)$ profile monotonically decreases with respect to $q$, and that $\tau(q)$ shows deviation from linearity indicating the presence of multifractality in all time series. Measures of the singularity spectra, $A$ have shown presence of structures (both smaller or larger) in the fluctuations; and $\Delta\alpha$ have shown weaker to stronger multifractality. The singularity spectra is fitted with p-model and we found weight parameter $p1$ to be different than $0.5$ which confirms multifractality present in data. Accounting non-zero dissipation factor suggests that energy distribution across the eddies to be non-uniform.

We now focus attention on the second experiment during which base of F region was moving upwards, thereby indicating possibility of PRE. We expected to find some different characteristics of this data owing to the fact PRE is the seeding mechanism for Rayleigh-Taylor instability. Of the six time series, three exhibited monofractal nature and remaining three showed weaker multifractality (considered in this study). $\Delta\alpha$ and skewness are found to be smaller compared to the first experiment. Singularity spectra for two time series are found to be left skewed with right truncated which shows time series has large structures but the spectrum is insensitive to smaller local fluctuations. But at altitude of $400.24$ km, the spectrum is found to be almost symmetrical, so may be this region has both large and small structures. Results for mean height of $348.99$ km are different than other two heights and evident for some different kind of physical mechanism which can be described by multiplicative cascade process. Though time series are characterized by weaker multifractality, these data has fractal behavior with long range correlation. However, we argue that more detailed study is required to reach any definite conclusion on the turbulent-like mechanism driving the ionospheric irregular structures.

Finally, we intend to test the potential of this algorithm in deciphering the morphology of the cascading phenomena. For this, we choose the first experiment where rocket intercepted a plasma bubble. Muralikrishna et al. (2003) reported presence of predominant sharp peaks in the power spectra over a wide range of heights, and they attribute these to a developing plasma bubble that subsequently dissipated energy, reaching an equilibrium which is evidenced by the absence of peaks. Our multifractal analysis has captured this sequence of events. Figure 5 show the variation of mean density and $\Delta\alpha$ with mean heights for the selected six time series on a 3-dimensional plane. Presence of a plasma bubble characterized by large scale irregularities, that in turn is reflected in the low density, is observed around a mean height of $292.37$ km. Contrarily, stronger multifractality is observed at this height. These inverse variation is in line with the turbulent like multiplicative cascade process. On the other hand, as the rocket traversed higher altitudes, the mean density increased while the multifractality became weaker. This suggests that the cascading process resulted in smaller scale irregularities by dissipating energy. Two dimensional plots showing

https://doi.org/10.5194/angeo-2019-133
Preprint. Discussion started: 25 October 2019


Annales Geophysicae Discussions
Open Access
EGU

the variation of mean density and $\Delta\alpha$ with mean heights are shown in the inset of Figure 5. We conclude at this point where we have presented the schematic hypothesis based on the multifractal analysis of the plasma irregularities in the ionospheric F region.

*Acknowledgements.* NJ is grateful to Dr. Anna Wawrzaszek for the discussion and guidance obtained on multifractal analysis and p-model. Data used in this analysis is available in the following repository: http://urlib.net/rep/8JMKD3MGP3W34R/3U8PQA8

https://doi.org/10.5194/angeo-2019-133
Preprint. Discussion started: 25 October 2019


Annales Geophysicae Discussions

## References

Abdu M.A., Nogueira P. A. B., Santos A. M., de Souza J. R., Batista I. S., and Sobral J. H. A.: Impact of disturbance electric fields in the evening on prereversal vertical drift and spread F developments in the equatorial ionosphere. Ann. Geophys., 36, 609-620, https://doi.org/10.5194/angeo-36-609-2018, 2018.

Alimov V.A., Vybornov F.I., Rakhlin A.V.: Multifractal Structure of Intermittency in a Developed Ionospheric Turbulence. Radiophys Quantum El, 51, 438, https://doi.org/10.1007/s11141-008-9044-4, 2008.

Bolzan M. J. A., Tardelli A., Pillat V. G., Fagundes P. R., and Rosa R. R.: Multifractal analysis of vertical total electron content (VTEC) at equatorial region and low latitude, during low solar activity. Annales Geophysicae,31, 127-133, https://doi.org/10.5194/angeo-31-127-2013, 2013.

Cander L. R.: Ionospheric Space Weather Targets, in: Ionospheric Space Weather. Springer International Publishing, 245-264, https://doi.org/10.1007/978-3-319-99331-7_9, 2019.

Chandrasekhar E., Prabhudesai S. S., Seemala G. K., and Shenvi N.: Multifractal detrended fluctuation analysis of ionospheric total electron content data during solar minimum and maximum. Journal of Atmospheric and Solar-Terrestrial Physics, 149, 31-39, https://doi.org/10.1016/j.jastp.2016.09.007, 2016.

Chian A. C., Abalde J. R., Miranda R. A., Borotto F. A., Hysell D. L., Rempel E. L., and Ruffolo D.: Multi-spectral optical imaging of the spatiotemporal dynamics of ionospheric intermittent turbulence. Scientific reports, 8, 10568, doi:10.1038/s41598-018-28780-5, 2018.

Dyrud L., Krane B., Oppenheim M., P/'ecseli H. L., Trulsen J., and Wernik A. W.: Structure functions and intermittency in ionospheric plasma turbulence. Nonlin. Processes Geophys., 15, 847-862, www.nonlin-processes-geophys.net/15/847/2008/, 2008.

Fornari, G., Rosa, R., De Meneses, F. C., and Muralikrishna, P.: Spectral fluctuation analysis of ionospheric inhomogeneities over Brazilian territory. Part I: Equatorial F-region plasma bubbles. Adv. Space Res., 58, 2037-2042, https://doi.org/10.1016/j.asr.2016.03.039, 2016.

de Freitas D. B., Nepomuceno M. M. F., de Moraes Junior P. R. V., Lopes C. E. F., Das Chagas M. L., Bravo J. P., Costa A. D., Canto Martins B. L., De Medeiros J. R., and Leão I. C.: New suns in the cosmos.III. Multifractal signature analysis. The Astrophysical Journal, 831, 87 https://doi.org/10.3847/0004-637x/831/1/87, 2016.

Grech D.: Alternative measure of multifractal content and its application in finance, Chaos, Solitons & Fractals, 88, 183–195, https://doi.org/10.1016/j.chaos.2016.02.017, 2016

Halsey T., Jensen M., Kadanoff L., Procaccial I., and Shraiman B.: Fractal measures and their singularities: The characterization of strange sets. Phys. Rev. A, 33, 1141-1151, 1986.

Ihlen Espen: Introduction to Multifractal Detrended Fluctuation Analysis in Matlab. Frontiers in Physiology, 3, 141, https://doi.org/10.3389/fphys.2012.00141, 2012.

Jahn J. M. and LaBelle, J.: Rocket measurements of high-altitude spread F irregularities at the magnetic dip equator. Journal of Geophysical Research: Space Physics, 103, 23427-23441, https://doi.org/10.1029/97JA02636, 1998.

Kantelhardt J., Zschiegner S., Koscielny-Bunde E., Havlin S., Bunde A., and Stanley H.: Multifractal detrended fluctuation analysis of nonstationary time series, Physica A: Statistical Mechanics and its Applications, 316, 87–114, 2002.

Kantelhardt, J. W., and Meyers, R. A. (Eds.): Fractal and multifractal time series, Encyclopedia of complexity and systems science, Springer New York, 3754–3779, https://doi.org/10.1007/978-0-387-30440-3_221, 2009.

Kelley M. C. and Hysell D. L.: Equatorial Spread-F and neutral atmospheric turbulence: a review and a comparative anatomy. Journal of Atmospheric and Terrestrial Physics, 53, 695-708 https://doi.org/10.1016/0021-9169(91)90122-N, 1991.

https://doi.org/10.5194/angeo-2019-133
Preprint. Discussion started: 25 October 2019




Kelley, M. C., Ilma R. R., and Crowley G.: On the origin of pre-reversal enhancement of the zonal equatorial electric field. Ann. Geophys., 27, 2053–2056, https://doi.org/10.5194/angeo-27-2053-2009, 2009.

Li G., Ning B., Liu L., Ren Z., Lei J., and Su S.-Y.: The correlation of longitudinal/seasonal variations of evening equatorial pre-reversal drift and of plasma bubbles. Annales Geophysicae, European Geosciences Union, 25 (12), 2008.

Lu X., Zhao H., Lin H., and Wu Q.: Multifractal Analysis for Soft Fault Feature Extraction of Nonlinear Analog Circuits. Mathematical Problems in Engineering, https://doi.org/10.1155/2016/7305702, 2016.

Macek W. M.: Multifractality and intermittency in the solar wind. Nonlin. Processes Geophys., 14, 695–700, 2007.

Makowiec D., Rynkiewicz A., Gałaska R., Wdowczyk-Szulc J., and Żarczyńska-Buchowiecka M.: Reading multifractal spectra: Aging by multifractal analysis of heart rate. Europhysics Letters, 94, 68005, https://doi.org/10.1209/0295-5075/94/68005, 2011.

Meneveau C. and Sreenivasan K.: Simple multifractal cascade model for fully developed turbulence. Physical Review Letters, 59, 1424-1427, 1987.

Miriyala S., Koppireddi P. R., and Chanamallu S. R.: Robust detection of ionospheric scintillations using MF-DFA technique. Earth, Planets and Space, 67, 98, https://doi.org/10.1186/s40623-015-0268-1, 2015.

Muralikrishna P., Vieira, L. P., and Abdu, M. A.: Electron density and electric field fluctuations associated with developing plasma bubbles, J. Atmos. Sol-Terr. Phy., 65, 1315-1327, https://doi.org/10.1016/j.jastp.2003.08.010, 2003.

Muralikrishna P. and Abdu, M. A.: Rocket measurements of ionospheric electron density from Brazil in the last two decades. Advances in Space Research, 37, 1091-1096, https://doi.org/10.1016/j.asr.2006.02.006, 2006.

Muralikrishna P. and Vieira L. P.: Equatorial F-region irregularities generated by the Rayleigh-Taylor instability mechanism: rocket observations from Brazil. Rev. Bras. Geof., 25, http://dx.doi.org/10.1590/S0102-261X2007000600016, 2007.

Neelakshi J., Rosa R. R., Savio S., De Meneses F. C., Stephany S., Fornari G., and Muralikrishna, P.: Spectral fluctuation analysis of ionospheric inhomogeneities over Brazilian territory. Part II: E-F valley region plasma instabilities. Advances in Space Research, 2019. https://doi.org/10.1016/j.asr.2019.07.015.

Peng C. K., Buldyrev S. V., Havlin S., Simons M., Stanley H. E., and Goldberger A. L.: Mosaic organization of DNA nucleotides. Phys. Rev. E, 49, 1685-1689, https://doi.org/10.1103/PhysRevE.49.1685, 1994.

Savio S., Muralikrishna P., Batista I. S., and de Meneses F. C.: Wave structures observed in the equatorial F-region plasma density and temperature during the sunset period. Advances in Space Research, 58, 2043-2051, http://dx.doi.org/10.1016/j.asr.2016.07.026, 2016.

Savio Odriozola S., De Meneses F. C., Muralikrishna P., Pimenta A., and Kherani E.: Rocket in situ observation of equatorial plasma irregularities in the region between E and F layers over Brazil, Ann. Geophys., 35, 413-422, https://doi.org/10.5194/angeo-35-413-2017, 2017.

Savio, S., Sousasantos, J., Pimenta, A. A., Yang, G., Kherani, E. A., Wang, C., and Liu, Z.: Quasiperiodic rising structures in the E-F valley region below the equatorial plasma bubble: A numerical study. Journal of Geophysical Research: Space Physics, 124, https://doi.org/10.1029/2019JA026620, 2019.

Sivavaraprasad G., Otsuka Y., Tripathi N. K., Chowdhary V. R., Ratnam D. V. and Khan M. A.: Spatial and temporal characteristics of ionospheric total electron content over Indian equatorial and low-latitude GNSS stations. Conference on Signal Processing And Communication Engineering Systems (SPACES), Vijayawada, 105-108. doi: 10.1109/SPACES.2018.8316326, 2018.

Tanna H. J., and Pathak K. N.: Multifractal behaviour of the ionospheric scintillation index time series over an Indian low latitude station Surat. Journal of Atmospheric and Solar-Terrestrial Physics, 109, 66-74, https://doi.org/10.1016/j.jastp.2014.01.009, 2014.

https://doi.org/10.5194/angeo-2019-133
Preprint. Discussion started: 25 October 2019




Telesca L. and Lovallo M.: Revealing competitive behaviours in music by means of the multifractal detrended fluctuation analysis: application to Bach's Sinfonias. Proc. R. Soc. A, 467, 3022-3032, https://doi.org/10.1098/rspa.2011.0118, 2011.

Wawrzaszek A. and Macek W. M.: Observation of the multifractal spectrum in solar wind turbulence by Ulysses at high latitudes. Journal of Geophysical Research, 115, 2010.

Wawrzaszek A., Echim M. and Bruno R.: Multifractal Analysis of Heliospheric Magnetic Field Fluctuations Observed by Ulysses. The Astrophysical Journal, 876:153, 1538-4357, 2019.

Wernik A. W., Secan J. A., and Fremouw E. J.: Ionospheric irregularities and scintillation. Advances in Space Research, 31, 971-981, https://doi.org/10.1016/S0273-1177(02)00795-0, 2003.

https://doi.org/10.5194/angeo-2019-133
Preprint. Discussion started: 25 October 2019


Annales Geophysicae Discussions
Open Access
EGU

**Table 1.** Multifractal analysis measures for first experiment : For time series at mean heights listed in first column, second column shows degree of multifractality ($\Delta\alpha$), third column gives the measure of asymmetry ($A$). Columns 4 to 6 lists the p-model fit parameters, $l1, p1, dp$ respectively.

| $< height >$ | degree of multifractality | measure of asymmetry | p-model fit parameters | | |
|---|---|---|---|---|---|
| (km) | $\Delta\alpha$ | $A$ | $l1$ | $p1$ | $dp$ |
| 264.58 | 0.53 | 0.82 | 0.5 | 0.364 | 0.059 |
| 270.22 | 0.82 | 1.11 | 0.5 | 0.340 | 0.065 |
| 292.37 | 0.93 | 2.99 | 0.5 | 0.339 | 0.02 |
| 324.00 | 0.72 | 0.32 | 0.5 | 0.315 | 0.090 |
| 358.56 | 0.52 | 0.37 | 0.5 | 0.360 | 0.070 |
| 429.65 | 0.28 | 0.51 | 0.5 | 0.399 | 0.0355 |

**Table 2.** Multifractal analysis measures for second experiment : For time series at mean heights listed in first column, second column shows degree of multifractality ($\Delta\alpha$), third column gives the measure of asymmetry ($A$). Columns 4 to 6 lists the p-model fit parameters, $l1, p1, dp$ respectively.

| $< height >$ | degree of multifractality | measure of asymmetry | p-model fit parameters | | |
|---|---|---|---|---|---|
| (km) | $\Delta\alpha$ | $A$ | $l1$ | $p1$ | $dp$ |
| 339.94 | 0.27 | 1.34 | 0.5 | 0.4230 | 0.012 |
| 348.99 | 0.22 | 1.72 | 0.5 | 0.4300 | 0.006 |
| 400.24 | 0.19 | 0.94 | 0.5 | 0.4335 | 0.01 |

https://doi.org/10.5194/angeo-2019-133
Preprint. Discussion started: 25 October 2019


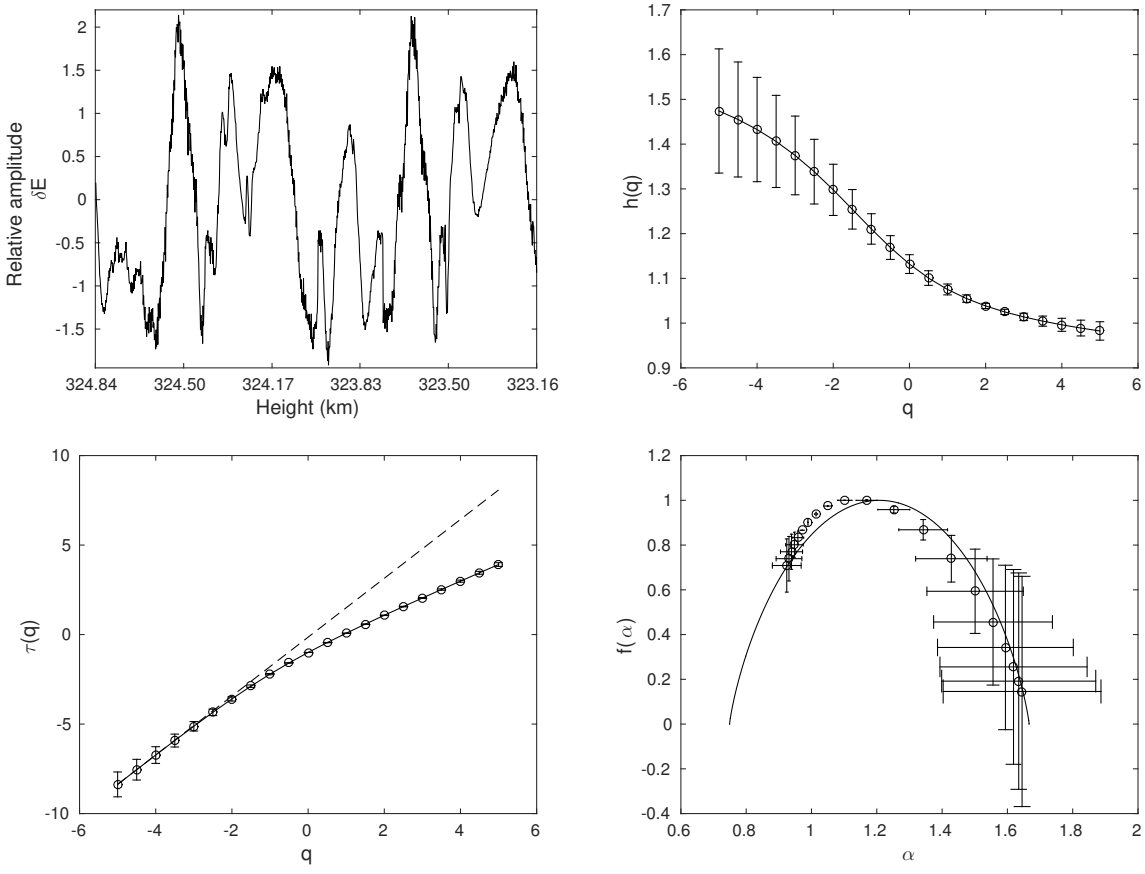


**Figure 1.** Comprehensive MFDFA for first experiment: upper panel, left figure shows time series at mean height 324.00 km and right figure shows $h(q)$ vs $q$ profile. Lower panel, left figure shows $\tau(q)$ vs $q$ profile along with dashed line which represent linear relationship between $\tau(q)$ and $q$, and right plot is of singularity spectrum fitted with p-model (continuous line).

https://doi.org/10.5194/angeo-2019-133
Preprint. Discussion started: 25 October 2019


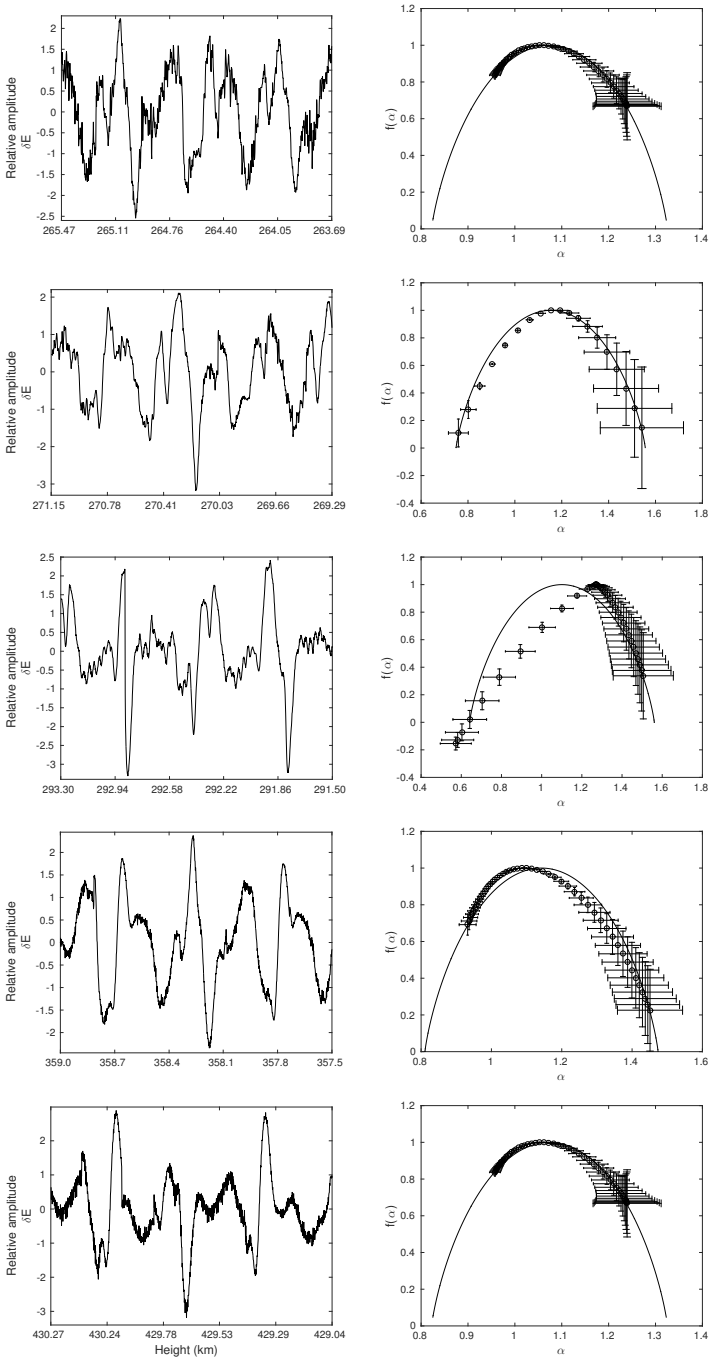


**Figure 2.** MFDFA for the first experiment: top to bottom panel show time series and its corresponding singularity spectrum with p-model fit (continuous line) for the mean heights of $264.58, 270.22, 292.37, 358.56$ and $429.65$ km respectively.

https://doi.org/10.5194/angeo-2019-133
Preprint. Discussion started: 25 October 2019


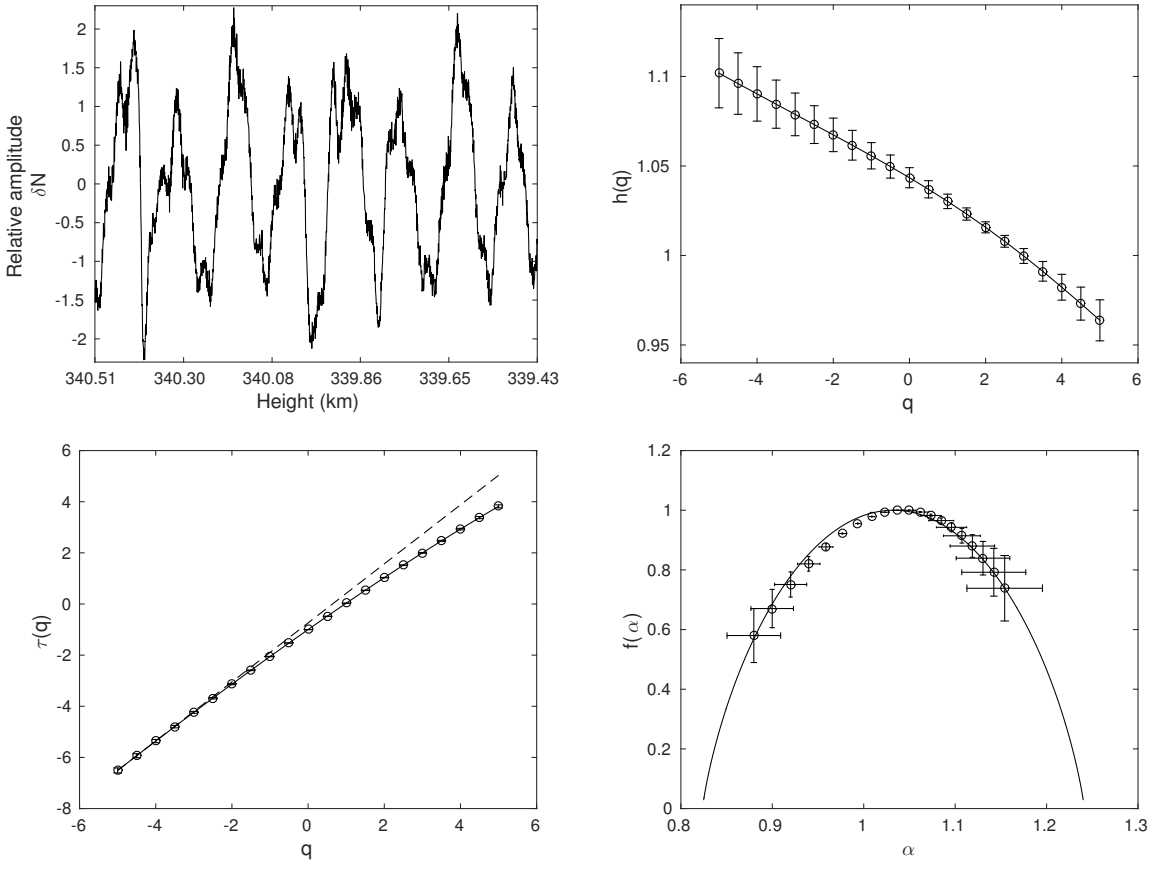


**Figure 3.** Comprehensive MFDFA for second experiment: upper panel, left figure shows time series at mean height 339.94 km and right figure shows $h(q)$ vs $q$ profile. Lower panel, left figure shows $\tau(q)$ vs $q$ profile along with dashed line which represent linear relationship between $\tau(q)$ and $q$, and right plot is of singularity spectrum fitted with p-model (continuous line).

https://doi.org/10.5194/angeo-2019-133
Preprint. Discussion started: 25 October 2019


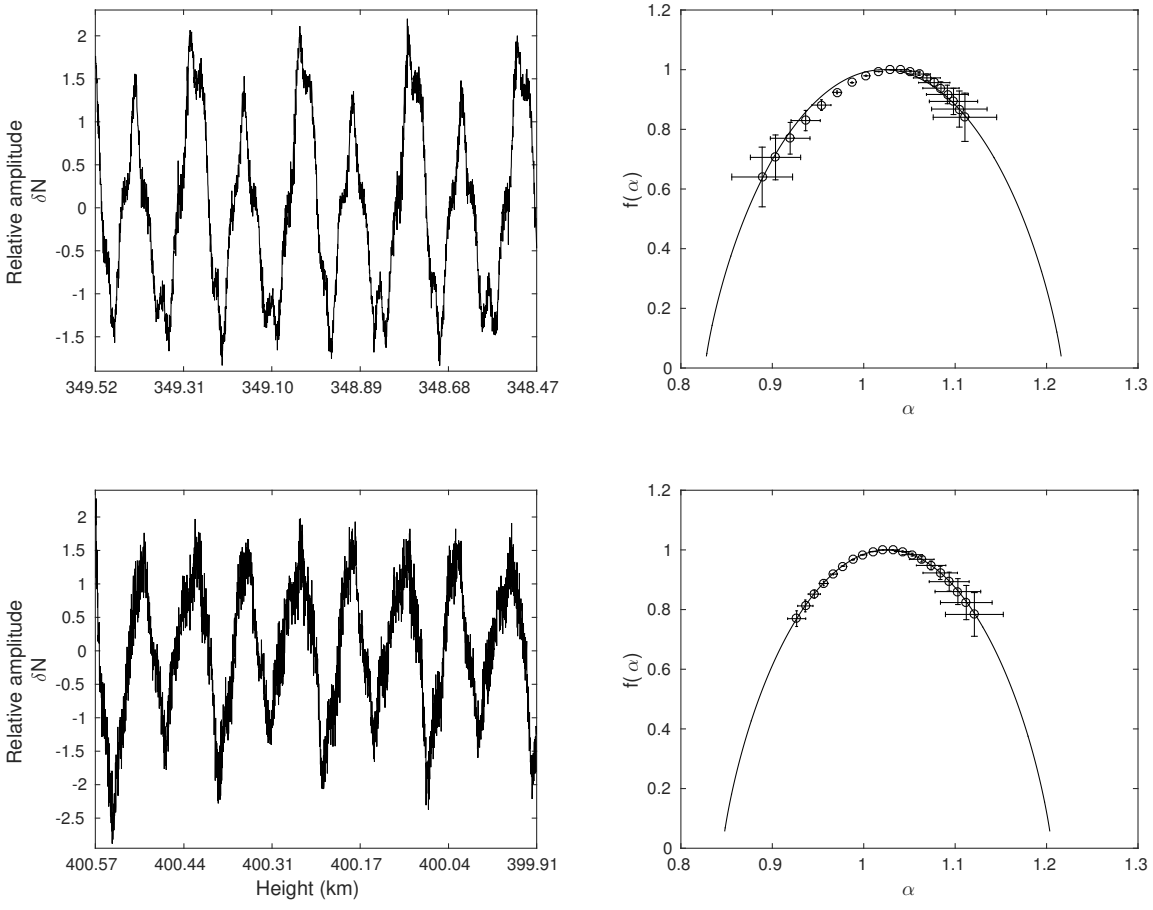


**Figure 4.** MFDFA for the second experiment: Upper panel shows multifractal analysis of time series at mean height 348.99 km and lower panel shows multifractal analysis of time series at mean height 400.24 km. In each panel the left plot shows time series for given mean height and right plot is of singularity spectrum fitted with p-model (continuous line).

https://doi.org/10.5194/angeo-2019-133
Preprint. Discussion started: 25 October 2019


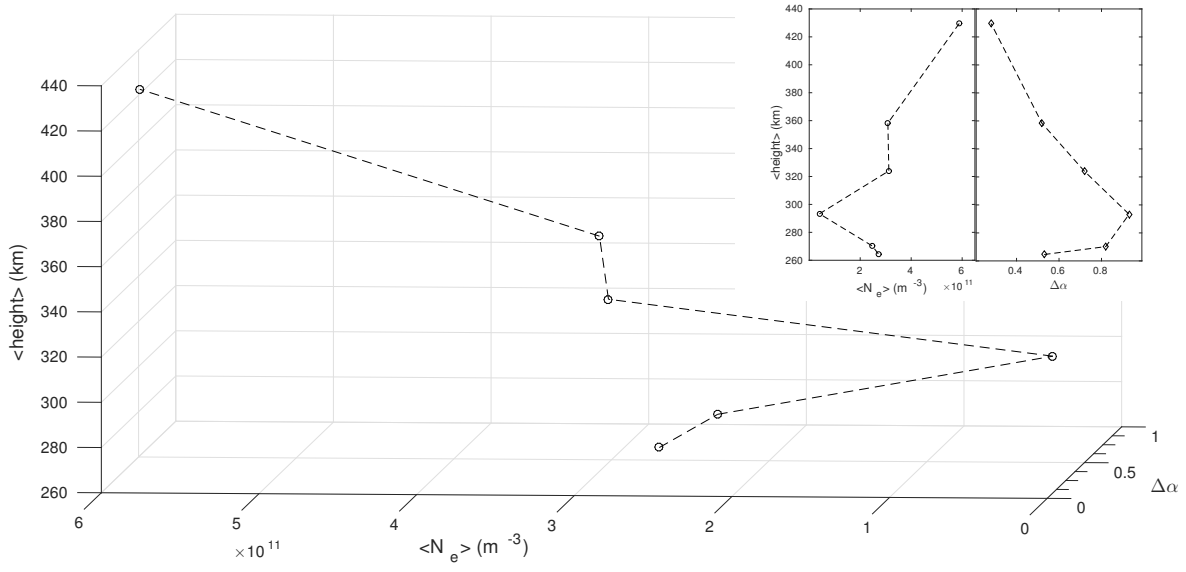


**Figure 5.** Variation of mean density and degree of multifractality with mean height for the selected six time series from the first experiment in 3-d plane. In the inset, these variations are shown in 2-d plane: of mean density (left) and degree of multifractality (right).